ACADEMIA ROMÂNĂ
Revue Roumaine de Chimie
http://web.icf.ro/rrch/

Rev. Roum. Chim.,
2017, *62*(10), 741-748

EFFECT OF GERMANIUM ADDITION ON THE STRUCTURAL AND TEXTURAL PROPERTIES OF BARIUM TITANATE, EVALUATION OF PHASE TRANSITION AND PHOTOCATALYTIC ACTIVITY

Mohamad KASSEM

Atomic Energy Commission of Syria, Chemistry Department, P.O.Box 6091-Damascus, Syria

Received March 17, 2017

This investigation deals with the changes that can occur in the structural and textural properties of barium titanate due the addition of different amounts of tetravalent element such as germanium. Phase transitions of $BaTiO_3$ have been also evaluated. Moreover, the focus was on the impact of the recorded changes on the photocatalytic activity of $BaTiO_3$ through the degradation of methyl red. Ge_xBaTiO_3 samples were prepared by solid state reaction, in air at 700°C, between germanium and barium titanate according to the molar ratio Ge/BT = 0.01, 0.05, 0.1, 0.2, 0.5, and 1. In order to study the effect of germanium addition to barium titanate, various techniques were used such as XRD, Micro Raman, FTIR, N2 Physisorption and UV-Vis spectrophotometer. The results showed a clear effect of the gradually added germanium on the structural and textural characteristics of $BaTiO_3$ .These effects include phase transition of $BaTiO_3$ from tetragonal phase to cubic one as well as the appearance of $BaGe_4O_9$ phase for the high germanium content samples. The results have revealed that the geometric and electronic changes as well as the phase composition have a noticeable influence on the photocatalytic activity of the Ge_xBaTio_3 samples where the degradation rate of methyl red has increased from about 0% (for pure $BaTiO_3$) to about 85% for Ge_xBaTiO_3 (Ge/BT=1). The increase in the photocatalytic activity was also enhanced by decreasing of the band gap, from 3.05 to 2.96 eV, due to the germanium addition.

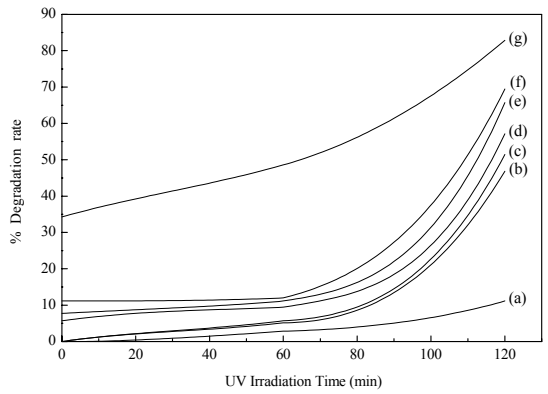

INTRODUCTION

Parallel with the industrial and technological progress in recent decades, it is indispensable to find the best ways to protect the environment and people's health from the waste produced by various industries, especially organic ones, which could be easily transmitted through water or air. It has been found through many researches that photocatalytic reactions using semiconductor materials is a promising solution for disposing of such wastes. [1-3]

The real investment of the photocatalytic degradation of organic pollutants requires unremitting efforts in order to get the appropriate materials for driving such processes.

Exploitation of the metal oxides semiconductors in photocatalysis were the basis of numerous scientific works which have revealed that some of these oxides showed a high photocatalytic activity, while the others were less effective because of the rapid recombination between electrons and holes (the most important parameter in the photocatalytic process). [4, 5]

* Corresponding author: cscientific@aec.org.sy

In order to reduce the recombination of e^- and h^+, great efforts have been devoted for amendment the properties of the used material (especially the band gap) through a doping process with another elements. Very encouraging results have been obtained in narrowing of the energy gap, which makes the material more effective. [6, 7]

Perovskite - type oxides have attracted a lot of attention because of the simple crystal structure, high stability, anisotropic optical behavior which qualifies them for use in many important applications such as photocatalysis process. The crystal structure of such oxides has the ability to host ions of different size, so the properties of these materials such as semi-conductivity as well as the microscopic characteristics (pore size distribution, surface area, grain size) can be adjusted by doping process or through forming solid solutions with other systems. [8, 9]

Transition metal titanate, particularly $BaTiO_3$ occupy an important position in the group of perovskite type materials because they can be formulated in several crystalline systems that provide a wide range of applications. [10, 11]

For the habilitation of this compound to be an effective photocatalyst it is important to narrow its band gap to less than 3.05 eV. For this purpose many doping works have been conducted using different elements such as Ni, Co, La, Fe, Mn, Nb etc. [12, 13]

In this work, we tried to make a comprehensive assessment of the effect of the germanium addition to barium titanate (BT). We also sought to explore the possibility to use the resulting materials in the photocatalytic applications such as the disintegration of the methyl red which is, to our knowledge, not carried out before.

EXPERIMETAL

Preparation of materials

With variable molar ratios Ge/BT = 0.01, 0.05, 0.1, 0.2, 0.5, and 1) the Ge_xBaTiO_3 powders have been prepared using the classical solid state reaction method. High-purity raw materials (germanium and commercial $BaTiO_3$) were weighed in appropriate proportions and homogenized in isopropyl alcohol in an agate mortar for 1 hour. The mixture has been heated, in air, for 7 hours at 700°C then it was slowly cooled up to room temperature, thereafter it was crushed and re-heated at 700°C; this operation was repeated 3 times.

Characterization methods

In order to track changes that may be caused by the addition of germanium to $BaTio_3$, a variety of advanced techniques were used: a transmission x-ray diffractometer model STOE STADI P ("STOE & Cie GmbH", Germany) operated at room temperature using Cu K_α radiation (λ = 0.154049 nm) and a linear PSD detector at 50kV and 30mA was used for the structural studies. The resulting patterns were measured between 5-90 degrees 2θ, with a step size of 0.02 degree.

The molecular structure and chemical bonding of the studied samples was performed using a micro-Raman spectrometer (Jobin Yvon, model Labram-800) ("Jobin Yvon Ltd.", UK) with 632 nm Helium Neon laser and a liquid-nitrogen Cooled CCD detector. Absorption bands were also recorded between 400 and 4000 cm-1 by a Fourier transform infrared (FT-IR) spectrometer in the transmittance mode (Bruker IFS66). All spectra were obtained at room temperature, using KBr discs containing 0.001g of the material to be studied.

A high speed gas sorption analyzer NOVA 2200 ("Quantachrome Corp.", USA), calibrated by a standard reference material of Al_2O_3, has been used for the surface area and pore structure measurements using BET [14] and BJH method.[15] All nitrogen adsorption-desorption isotherms were performed at liquid nitrogen.

Ultraviolet-visible absorption spectra were collected at room temperature in the range 200–800 nm using AvaSpec-2028 Fiber Optic spectrometer ("Avantes B.V.", Holland). The band gap energies related to studied materials were determined using following equation: Band gap energy (eV) = 1240 / wavelength (nm).

For the photocatalysis studies, 200 mg of the concerned material was suspended in 200 ml methyl red aqueous solution (30 mg/L). The suspension has been irradiated, at room temperature with constant stirring, using a commercial 20W UV lamp as a light source. In each run, the concentration of the methyl red in the solution was measured three times per hour at λmax =506 nm, using UV-Spectrophotometer UV-3101 PC ("Shimadzu", Japan). The degradation rate was calculated using the formula:

$$(\text{Degradation rate } (\%) = [(C0-C)/C0] \times 100) \approx \approx [(A0-A)/A0] \times 100)$$

where C0 is the initial concentration of methyl red, C is the concentration at time t and A is the absorbance.

RESULTS AND DISCUSION

XRD Measurements

In order to study the effect germanium addition on the crystal structure of $BaTiO_3$, X-ray diffraction patterns were recorded at room temperature for pure $BaTiO_3$ and Ge_xBaTiO_3 specimens as it is shown in Fig.1. The diffraction peaks of the pure $BaTiO_3$ (Fig.1 *a*)) match well with those characteristics of the tetragonal phase (JCPDS card 89-1428).

In the low concentration range of germanium $0 \leq Ge/BT \leq 0.1$, the samples exhibit a single phase related to the tetragonal $BaTio_3$. This indicates that when a small amount of germanium is added, within the mentioned range, the substitution process in (Ti) sites inside the BaTiO3

lattice could occur without deformation of the original structure.

By increasing the germanium concentration, molar ratio Ge/BT >0.1, a significant decrease in the intensities of the diffraction peaks related to $BaTiO_3$ were monitored (Fig.1 (*b to g*)).This could be interpreted as a partial destruction of the structure of this compound. It was found also that the decrease in relative intensity was accompanied by the appearance of new diffraction peaks at 2θ values: 24.1, 30.8, and 32.6 degree which could be assigned to the phase $BaGe_4O_9$ (JCPDS card 87-1989).The formation of this new phase could be attributed to the increase in the substitution of Ge^{4+} (ionic radius 0.054nm) for Ti^{4+} (ionic radius 0.0605 nm).

For the highest germanium content, Ge/BT = 1, an asymmetrical peak broadening has been observed (Fig.2 *g*), which is probably a result of the coexistence of cubic and tetragonal phases (JCPDS card 89-2475), (JCPDS card 89-1428) respectively.

In this context, it should be noted that no peak belonging to the pure germanium has been detected in any of the diffraction patterns.

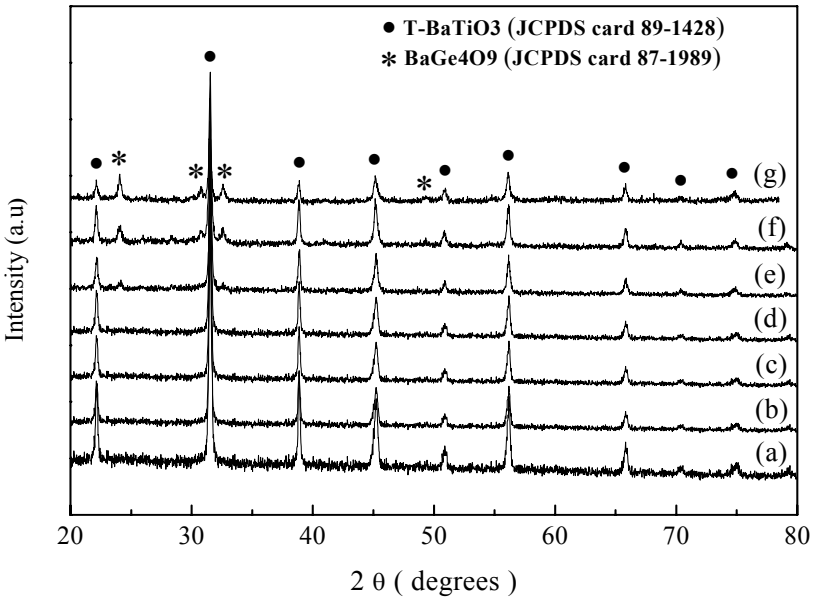

Fig. 1 – XRD patterns for pure $BaTiO_3$ (*a*) And Ge_xBaTiO_3 samples where: x= 0.01 (*b*) 0.05 (*c*) 0.1(*d*) 0.2 (*e*) 0.5 (*f*) and 1 (*g*).

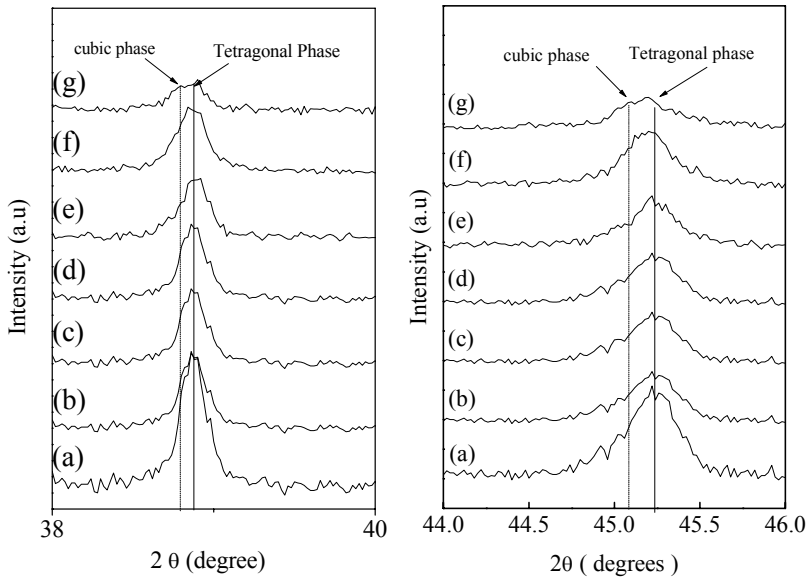

Fig. 2 – XRD patterns, in the ranges $2\theta = 36 - 38^\circ$ and $2\theta = 44 - 46^\circ$ for pure $BaTiO_3$ (*a*) And GexBaTiO3 samples where: x= 0.01 (*b*) 0.05 (*c*) 0.1(*d*) 0.2 (*e*) 0.5 (*f*) and 1 (*g*).

Table 1

Phase composition of Ge_xBaTiO_3 samples 0< x = Ge/BT <1

Molar ratio Ge/BT	BT-Tetragonal Phase (%)	$BaGe_4O_9$ (%)	BT-Cubic Phase (%)
0	100	0	0
0.01	100	0	0
0.05	100	0	0
0.1	100	0	0
0.2	92	8	0
0.5	82	18	0
1	50	30	20

The phase compositions, related to the studied samples, are listed in Table 1. This quantitative phase analysis was executed from the diffraction patterns using WinXpow 32 Software, which is based on the reference intensity ratio method (RIR) and stored I/Icor values for identifying phase.

Raman spectroscopy

In order to prove the phase transition of $BaTiO_3$ from tetragonal to cubic which has been mentioned during the discussion of the XRD results; and based on the fact that the diffraction patterns of these two structures are very similar where the distinction between them is so strenuous, it was necessary, for providing more information about these transformations, to use another techniques.

Materials scientists generally consider that the Raman scattering spectroscopy is one of the most suitable procedures for the detection of changes in atomic structure and phase transitions of substances. In this context, Raman spectra, for pure $BaTiO_3$ and Ge_xBaTiO_3 samples, were recorded (Fig. 3).

In accordance with the relevant literature, all peaks observed in (Fig.3 *a*) could be assigned to the tetragonal $BaTiO_3$ optical mode. [16, 17] These peaks become more expansive and less intense by increasing the incorporation of the germanium atoms in molar ratios up to 0.1. Such results, which are in harmony with those obtained by XRD, could be attributed to the decrease in the tetragonal structural stability.

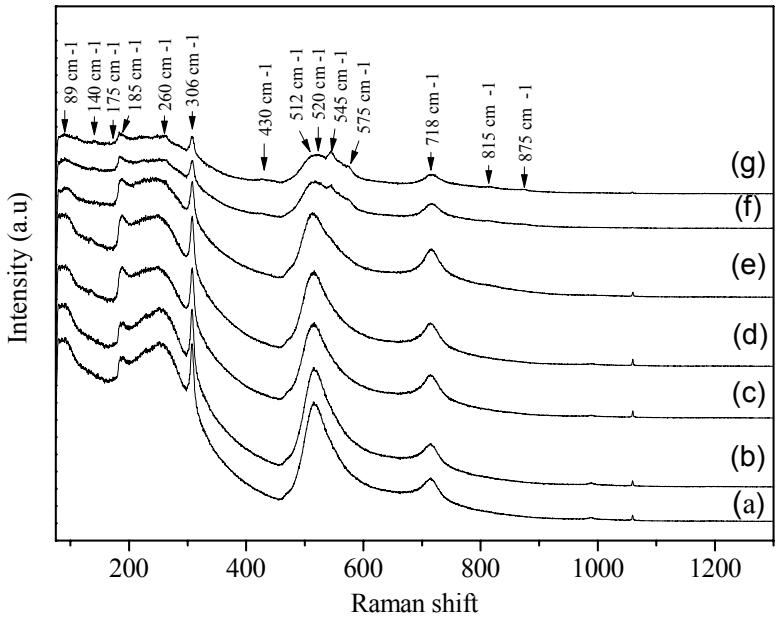

Fig. 3 – Micro-Raman Spectra for pure $BaTiO_3$ (*a*) and GexBaTiO3 samples where : x= 0.01 (*b*) 0.05 (*c*) 0.1(*d*) 0.2 (*e*) 0.5 (*f*) and 1 (*g*).

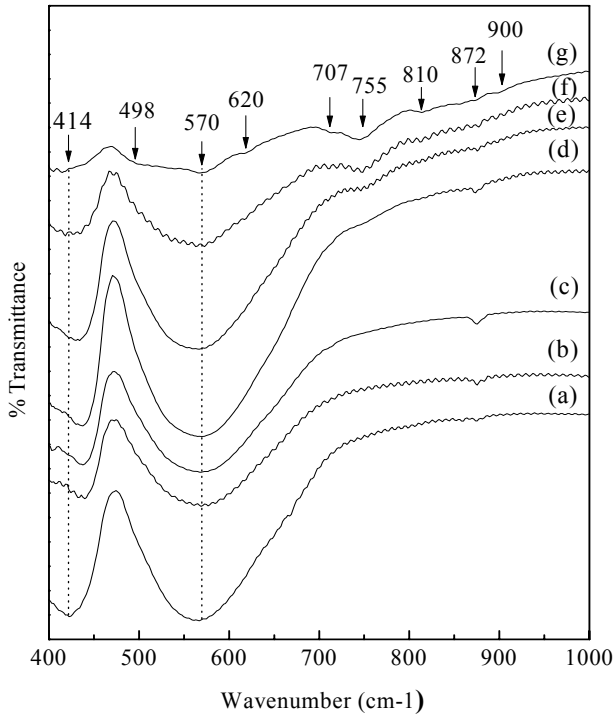

Fig. 4 – FT-IR spectra for pure $BaTiO_3$ (*a*) and Ge_xBaTiO_3 samples where : x= 0.01 (*b*) 0.05 (*c*) 0.1(*d*) 0.2 (*e*) 0.5 (*f*) and 1 (*g*).

For the highly doped Ge_xBaTiO_3 samples, x > 0.1, the expansion and decline in intensity of Raman peaks remain incessant, but some tetragonal features still noticeable, albeit weakly, as evidenced through the presence of the peaks at 306 ,520 and 718 cm^{-1} which are the fingerprint for this phase (Fig.3 *g*). The Raman spectra of this group of samples also show the presence of new peaks at 430, 545, 575, 815 and 875 cm^{-1} which are characteristic of the $BaGe_4O_9$ phase. [18]

Furthermore, with regard to this type of samples, the peak broadening was accompanied by an emergence of new peaks at 185, 260, and 512 cm^{-1}, which may be an indicative of the presence of cubic phase of the $BaTiO_3$.[19, 20] These results coincide well with those obtained by XRD.

Fourier transform infrared (FT-IR)

To get to more indications about the changes of the atomic structure of $BaTiO_3$, announced by XRD and Raman spectroscopy, FT-IR spectra of Ge_xBaTiO_3 were recorded as shown in Fig. 4.

For the pure $BaTiO_3$,the most distinctive infrared bands are situated around 421 cm^{-1} and 564 cm^{-1} which are related respectively to the bending normal vibrations of Ti-O bond and stretching vibrations of TiO_6 octahedron connected to the barium ion in the crystalline $BaTiO_3$.[21, 22]

FTIR spectra related to Ge_xBaTio_3 samples (0<x< 0.1) exhibit the same behavior of that relating to the pure $BaTiO_3$, the only difference, that has been monitored, was the broadening of the peaks and lowering of their intensities.

With respect to the samples containing higher amounts of germanium, x > 0.1, a new peak started to appear at about 750 cm^{-1} which referred to the development of a new phase identified as $BaGe_4O_9$.[23]

For the sample with highest content of germanium, Ge/BT =1 , the FTIR spectrum reveals the existence of weak intensity peaks at 421 and 564 cm^{-1}, related to the tetragonal $BaTiO_3$; these peaks were accompanied with the emergence of other ones at 575, 620, and 755 cm^{-1} indicating the development of $BaGe_4O_9$ phase. In addition the spectrum showed also small peaks at 498, 707, 810, 872 and 900cm^{-1} which could be related to the cubic phase of $BaTiO_3$.[24]

N_2 adsorption-desorption measurements

Complementing to investigate the changes occurred on $BaTiO_3$ due to the addition of germanium, it was helpful to highlight some of the textural characteristics such as surface area and pore properties using nitrogen adsorption measurements which are widely utilized for this purpose. The results of this course of action are assembled in Fig. 5.

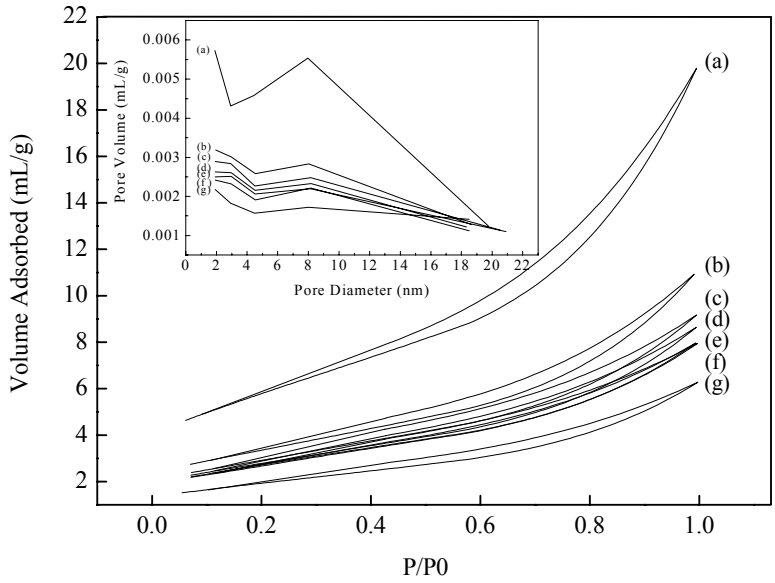

Fig. 5 – Nitrogen adsorption-desorption isotherms and pore size distributions for pure $BaTiO_3$ (*a*), Ge_xBaTiO_3 where x= 0.01 (*b*) 0.05 (*c*) 0.1(*d*) 0.2 (*e*) 0.5 (*f*) and 1 (*g*).

Table 2

Textural Properties derived from N2 adsorption-desorption measurements for pure $BaTiO_3$ and Ge_xBaTiO_3 samples

Molar Ratio Ge/BT	Surface area (m^2/g)	Pore Volume (mL/g)	Pore Diameter (nm)
0	20.32	0.031	6.0
0.01	11.8	0.017	5.7
0.05	10.35	0.014	5.5
0.1	9.8	0.013	5.6
0.2	9.65	0.012	5.6
0.5	9.5	0.012	5.6
1	7	0.010	5.7

All isotherms, related to the pure $BaTiO_3$ or to Ge_xBaTiO_3 samples, almost show the type V with the presence hysteresis loop which indicate that these samples have a mesopore structure. [25] It can be seen also that, in the high pressure region, the isotherms become less curvature by increasing the amount of germanium. This phenomenon could be related to the formation of micropores resulting from the presence of $BaGe_4O_9$ which generate a disordering in the $BaTio_3$ mesoporosity .This imperfection of the mesoporosity has been confirmed through the measuring of the pore size distribution which becomes more broadening with increasing the germanium content.

BET surface areas and pore properties of pure $BaTio_3$ and the germanium-doped samples are shown in Table 2.

Photocatalytic Activity

Taking into account the results obtained for above, which clearly showed some changes in the properties of $BaTiO_3$ that induced by the addition of different quantities of germanium, the question arises: Is it possible to use the resulting materials as catalysts. The photocatalytic activities, of pure and doped $BaTio_3$, were evaluated through the degradation of methyl red under UV irradiation.

Fig. 6 shows the photocatalytic degradation of methyl red as function of irradiation time for pure and doped $BaTio_3$ samples. It is clearly seen that the photocatalytic activity of the pure $BaTiO_3$ is very low and almost non-existent. When germanium is added gradually, the degradation rate begins increasing, especially after a long time of irradiation, until it achieves 85% for samples with the highest content of germanium (Ge/BT = 1). The enhancement of the photocatalytic activity for these samples could be attributed to the lowering of the band gap which was ranging from 3.05 eV (for the pure $BaTiO_3$), to 2.96 eV (for the highest germanium content sample; Ge/BT = 1).

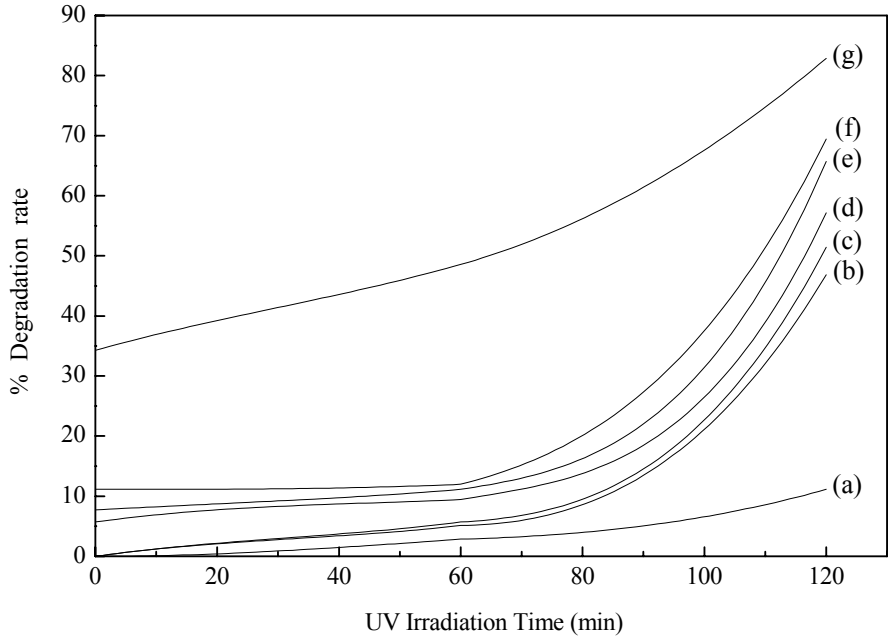

Fig. 6 – Photocatalytic degradation rate under UV irradiationof Methyl Red solution in the presence of : pure $BaTiO_3$ (*a*), Ge_xBaTiO_3 where : x= 0.01 (*b*) 0.05 (*c*) 0.1(*d*) 0.2 (*e*) 0.5 (*f*) and 1 (*g*).

Furthermore, this increment in activity may be linked also to the geometric factor where a clear deformation in the crystal structure of $BaTio_3$ has been detected for the high germanium content samples. It is also possible that phase composition of these samples, which includes several crystalline phases, has contributed to the increase in catalytic activity.

CONCLUSION

The incorporation of different quantities of germanium in barium titanate has been performed through solid state method. Analyzing the results obtained by several techniques revealed a considerable influence of the germanium on the structural and textural properties. The results showed that, for the low germanium content samples, the tetragonal structure of $BaTio_3$ was disturbed by the appearance of a new phase identified as $BaGe_4O_9$. In addition to the existence of this compound, a phase transition of $BaTiO_3$ from tetragonal to cubic phase has been detected for the high germanium content samples. The results revealed also that the germanium ions have affected the electrical properties of $BaTiO_3$ where the band gap dropped from 3.05 to 2.96 eV.

All the structural, textural and electrical changes have influenced the photocatalytic activities of the Ge_xBaTiO_3. This effect has appeared clearly through the enhancement of the degradation rate of methyl red from about 0% (for the pure $BaTiO_3$) to about 85% for the highly doped sample (Ge/BT = 1).

Acknowledgement: The author would like to thank Professor I. Othman, Director General and Dr. Z. Ajji, Head of the Chemistry Department for their encouragement. Thanks are also to Mr. H.Harmalani for assistance in the experimental works as well as J. Abuhilal and A. Al-Zier and for the spectroscopic measurements.

REFERENCES

1. L. Das, M. Dutta and J. K. Basu, *Inter. J. Environ.Sci.,* **2013**, *4*, 415 - 431.
2. F. Hashemzadeh, R. Rahimi and A. Gaffarinejad, *Int. J. Appl. Chem. Sci. Res.*, **2013**, *1*, 95-102.
3. C. W. Lai, J. C. Juan, W. B. Ko and S. B. A. Hamid, *Int. J. Photoenergy*, **2014**, *2014*, doi. 10.1155/2014/524135.
4. D. T. Dimitrov, M. M. Milanova and R. P. Kralshevska, *Bulg. Chem. Commun.*, **2011**, *43*, 489 - 501.
5. K. Maeda and K. Domen, *J. Phys. Chem. C*, **2007**, *111*, 7851-7861.
6. A. I. Kokorin , V. M. Arakelyan and V. M. Arutyunian, *Russ.Chem.Bull., Int. Ed.*, **2003**, *52*, 93—97.
7. S. I. Mogal, M. Mishra1, V. G. Gandhi and R. J. Tayade, *Mate. Sci. Forum*, **2013**, *734*, 364-378.
8. J. R. Mawdsley and T. R. Krause, *Appl. Catal. A: General*, **2008**, *334*, 311–320.
9. M. Popaa, L. V. Hong and M. Kakihana, *Physica B*, **2003**, *327*, 233–236.
10. W. W. Lee, W.-H. Chung, W.-S. Huang, W.-C. Lin, W.-Y. Lin, Y.-R. Jiang and C.-C. Chen, *J. Taiwan Inst. Chem. Eng.*, **2013**, *44*, 660–669.
11. X. Xiong, R. Tian, X. Lin, D. Chu and S. Li, *J. Nanomater.*, **2015**, *2015*, 1-6.

12. D. Hreniak, E. Łukowiak, K. Maruszewski, R. Pązik and W. Stręk, *Mater. Sci. Forum*, **2002**, *20*, 43-50.
13. T. K. Kundu, A. Jana and P. Barik , *Bull. Mater. Sci.,* **2008**, *31*, 501–505.
14. J. C. Groen, L. A. A. Peffer and J. Perez-Ramırez, *Microporous Mesoporous Mater.*, **2003**, *60*, 1–17.
15. K. Sing, *Colloids Surf. A: Physicochem. Eng. Aspects*, **2001**, *187-188*, 3–9.
16. A. Garrido-Hernández, A. García-Murillo, F. D. J. Carrillo-Romo, L. A. Cruz-Santiago, G. Chadeyron, A. D. J. Morales-Ramírez and S. Velumani, *J. Rare Earths,* **2014**, *32*, 1016-1021.
17. H.-W. Lee, S. Moon, C.-H. Choi and D. K. Kim, *J. Am. Ceram. Soc.*, **2012**, *2012*, 1-6.
18. Y. Takahashi, K. Iwasaki, H. Masai and T. Fujiwara, *J. Ceram. Soc. Japan*, **2008**, *116*, 1139-1142.
19. S. Adireddy, C. Lin, B. Cao, W. Zhou and G. Caruntu, *Chem. Mater.*, **2010**, *22*, 1946–1948.
20. E. Chávez, S. Fuentes, R. A. Zarate and L. Padilla-Campos, *J. Mol. Struct.*, **2010**, *984*, 131–136.
21. A. A. Aal, T. R. Hammad, M. Zawrah, I. K. Battisha and A. B. A. Hammad, *Acta Phys. Pol. A* **2014**, *126*, 1318-1321.
22. S. Hao, D. Fu, J. Li, W. Wang and B. Shen, *Int. J. Inorg. Chem.*, **2011**, doi:10.1155/2011/837091.
23. A. Margaryan, "Ligands and Modifiers in Vitreous Materials: Spectroscopy of Condensed Systems", Singapore: World scientific publishing co. Pte. Ltd. 1999.
24. M. Garcıa-Hernandez, G. Chadeyron, D. Boyer, A. Garca-Murillo, F. Carrillo-Romo and R. Mahiou, *Nano-Micro Lett.*, **2013**, *5*, 57-65.
25. W. Jiang, C. Jiang, X. Gong and Z. Zhang, *J. Sol-Gel Sci. Technol.*, **2009**, *52*, 8–14.